Crystallization via tubing microfluidics permits both in situ and ex situ X-ray diffraction

Charline J. J. Gerard, Gilles Ferry, Laurent M Vuillard, Jean A Boutin, Léonard M.G. Chavas, Tiphaine Huet, Nathalie A Ferte, Romain A Grossier, Nadine Candoni, Stéphane Veesler

Crystallization via tubing microfluidics permits both in situ and ex situ X-ray diffraction

Charline J.J. Gerard[1], Gilles Ferry[2], Laurent M. Vuillard[2], Jean A. Boutin[2], Leonard M.G. Chavas[3], Tiphaine Huet[3], Nathalie Ferte[1], Romain Grossier[1], Nadine Candoni[1], Stéphane Veesler*[1]

[1]CINaM - CNRS, Aix-Marseille Université, Campus de Luminy, Case 913, F-13288 Marseille Cedex 09 fax : +334 91418916, email : veesler@cinam.univ-mrs.fr

[2]Institut de Recherches SERVIER, 125, chemin de ronde, F-78290 Croissy-sur-Seine.

[3]Synchrotron SOLEIL Proxima-I, Gif-sur-Yvette, France

ABSTRACT.

We used a microfluidic platform to address the problems of obtaining diffraction quality crystals and crystal handling during transfer to the X-ray diffractometer. We optimize crystallization conditions of a protein of pharmaceutical interest and collect X-ray data both in situ and ex situ.

1. Introduction

Structural biologists need to solve three-dimensional structures of biological macromolecules via X-ray crystallography. Two decisive and rate-limiting steps are obtaining diffraction-quality crystals and handling crystals during transfer to the diffractometer.

Obtaining diffraction-quality crystals is complex and influenced by many parameters (pH, temperature, types of buffer, salts and crystallization agents). Problems in producing suitable crystals can be tackled in two steps: first, screening for favourable crystallization conditions in the phase diagram and second, optimizing crystal growth by developing a specific kinetic path in the phase diagram. Screening is an expensive task, both in terms of time and raw materials. Moreover, when only small quantities of sample materials are available, a suitable experimental tool is essential. Microfluidic techniques, i.e. the control and manipulation of flows at sub-millimetre scale using miniaturized devices called Lab On Chip (LOC)(van der Woerd *et al.*, 2003) are appropriate for automating, miniaturizing and high-throughput crystallization approaches involving multiple operations such as mixing, analysis, separation(Leng J. & Salmon J.B., 2009). LOCs are applied in both fast screening and optimization stages of protein crystallization studies, via the integration of traditional protocols of protein crystallization(Candoni N. *et al.*, 2012). Furthermore, the microfluidics approach suits the stochastic nature of nucleation(Hammadi *et al.*, 2015) because it allows multiple independent experiments.

Manual handling of the sample crystals can mechanically and environmentally stress them. The stress induced during this delicate step may affect crystal quality and decrease its diffractive power. To minimize manual handling, an alternative is in situ X-ray data collection. One approach involves using X-ray-transparent microfluidic devices(Hansen *et al.*, 2006, Dhouib *et al.*, 2009, Stojanoff *et al.*, 2011, Guha *et al.*, 2012, Pinker *et al.*, 2013, Khvostichenko *et al.*,

2014, Horstman *et al.*, 2015, Heymann *et al.*, 2015, Maeki *et al.*, 2015). Another solution, following Yadav's pioneering work(Yadav *et al.*, 2005), is to collect X-ray data directly in micro capillary(Li *et al.*, 2006, Maeki *et al.*, 2012). For ex situ data collection, Gerdts(Gerdts *et al.*, 2010) and Stojanoff(Stojanoff *et al.*, 2011) harvested a protein crystal from a microfluidic chanel using a cryo-loop and Li (Li *et al.*, 2006) made crystals flow out of a capillary, then looped and flash-froze them.

We present an application that addresses these two problems using a microfluidic platform developed in our group(Zhang *et al.*, 2017). We apply our platform to the crystallization of a protein of pharmaceutical interest, human Quinone Reductase 2 (QR2 EC 1.10.5.1), involved in Alzheimer disease (Hashimoto & Nakai, 2011), Parkinson disease (Fu *et al.*, 2008) and oxidative stress (Nosjean *et al.*, 2000). We optimize crystallization conditions of QR2 and collect X-ray data both in situ and ex situ to characterize the crystals obtained.

2. Optimization and crystallization results using the microfluidic platform

The microfluidic platform developed in our group offers four modular functions (Zhang *et al.*, 2017): droplet formation, on-line UV characterization, incubation and observation (figure 1). The microfluidic device is built using commercially-available PEEK junctions and Teflon tubing, initially designed for high-performance liquid chromatography systems rendering it compatible with all solvents, simple, cheap, flexible and easily incorporated into any laboratory. We adapt the platform to generate droplets of 2nL in long Teflon tubing (150µm ID from IDEX Health and Science), without using surfactant (Zhang *et al.*, 2015). Droplets are generated by crossing a continuous phase (FC70 fluorinated oil from Hampton research) with dispersed phases (containing the protein and the crystallization agent(s)) in a microfluidic junction (Te, cross or 7-entry junction from IDEX Health and Science according to experimental requirements). A programmable syringe pump (neMESYS, cetoni GmbH) controls the flow-rates of the different fluids. We couple an on-line UV detector (USB2000+, Ocean optics) to the Teflon tubing after the droplet formation zone ((3) in figure 1) using an home-made and specially-designed UV cell. (Zhang *et al.*, 2017) The tubing wall material is transparent enough under UV light. Thus, allowing real-time acquisition, in-situ spectral analysis of droplets is possible: absorbance at one or several wavelengths can be recorded. Hence, the evolution of the chemical composition gradient, in a group of generated droplets with identical size, can be analyzed using Beer-Lambert's law.

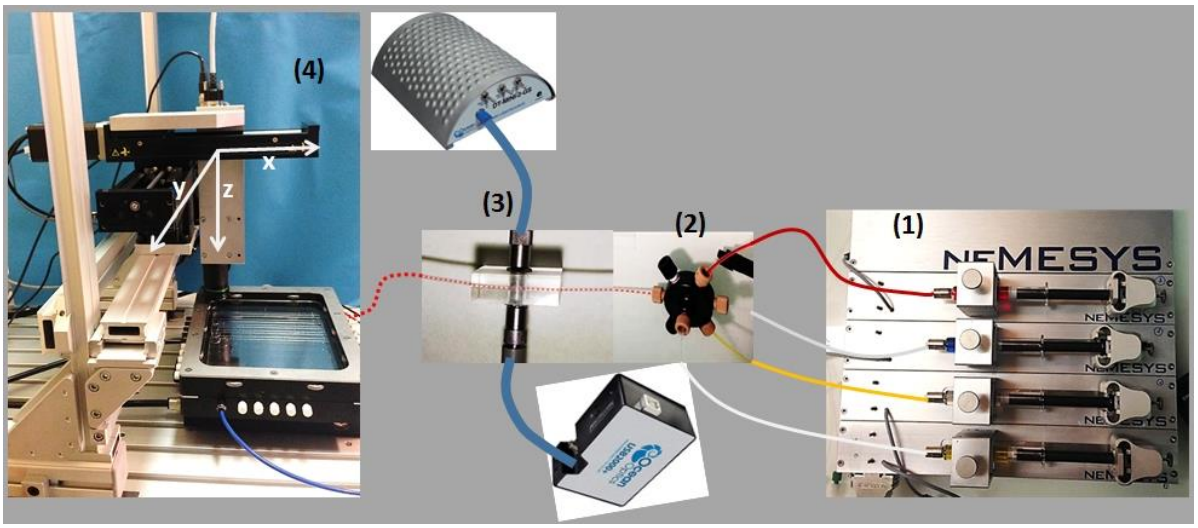

Figure 1. Pictures of the home-made microfluidic platform: (1) syringe pump, (2) 7-entry junction, (3) on-line UV module (4) tubing-holder for thermostatting and observation with XYZ-motorized camera.

Experimental conditions are based both on solubilities obtained by equilibrating crystal-solution suspensions over time (figure 1, Supplementary Information) and crystallization conditions used for structural determination (Foster *et al.*, 1999). Subsequent gradient optimization, using experimental conditions presented in figure 2, provides optimal conditions leading to high quality crystals. At least 60 droplets of 2nL per experimental conditions were generated and observed (figure 2). Crystals in droplets from experiment (b) (figure 2) were used for X-ray diffraction (XRD).

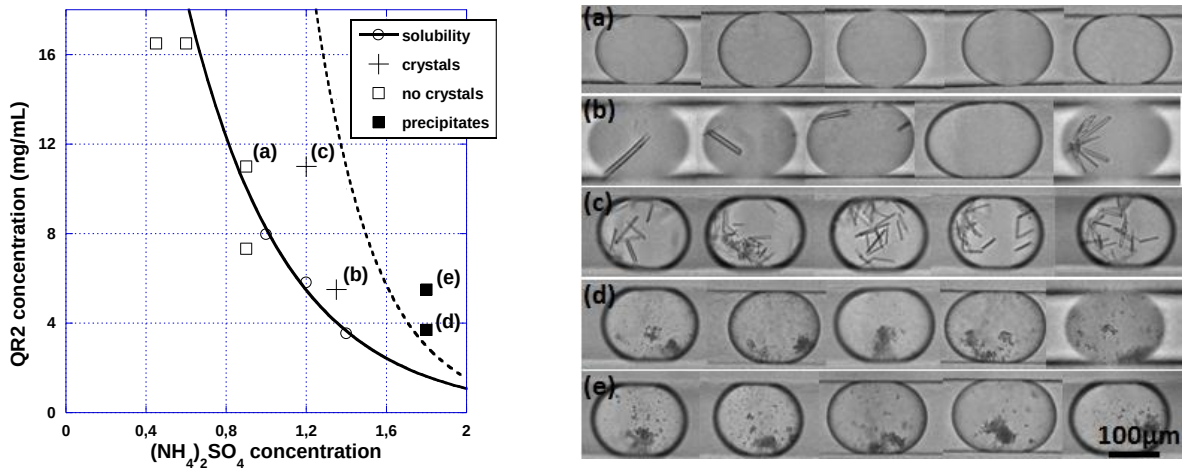

Figure 2. Solubility of QR2 versus $(NH_4)_2SO_4$ at pH=8 (20mM Tris-HCl and 150mM NaCl – error bars have the size of the markers), and the different experimental conditions tested in the fine-gradient experiment. The dashed line is a guide for the eye to separate the crystallization and precipitation zones. Photos of 5 representative droplets obtained in 2nL droplets in Teflon capillary (150µm ID) after 24h. (a) 11 mg/mL QR2, 0.9M $(NH_4)_2 SO_4$, (b) 5.5 mg/mL QR2, 1.35M $(NH_4)_2 SO_4$, (c) 11 mg/mL QR2, 1.2M $(NH_4)_2 SO_4$, (d) 3.7 mg/mL QR2, 1.8M $(NH_4)_2 SO_4$, (e) 5.5 mg/mL QR2, 1.8M $(NH_4)_2 SO_4$, at 20°C.

3. XRD characterization

Although direct X-ray data collection from the microfluidic devices is used to minimize manual handling, Teflon-related background noise is significant on diffraction patterns. This may reduce the quality of the diffraction data (Yadav *et al.*, 2005) and strongly reduce the observed diffraction limits of the crystals. Hence, we tested two approaches: (1) transferring droplets containing the crystals of interest from Teflon to silica tubing for in situ XRD without freezing; and (2) extracting the crystals of interest from the tubing, depositing them on a MicroMesh™, a polyimide grid transparent to X-rays, for ex situ XRD thereby avoiding mechanical shocks.

3.1. In situ XRD. We transferred the droplets from experiment (b) of figure 2, performed in Teflon tubing, to silica tubing (fused silica tubing with a polyimide coating -150µm ID, 360µm OD, from IDEX health and science) using a linear junction (IDEX health and science). The internal silica tubing wall was coated with a commercial hydrophobic surface-coating agent (Aquapel®, PPG industry)(Mazutis *et al.*, 2009) to ensure droplet stability. The silica tubing containing the droplets was directly mounted on a magnetic base extracted from standard SPINE sample loops, ready for transfer to the X-ray setup (figure 3). For the proof of concept, a single crystal was analysed by XRD at room temperature on the beam line PROXIMA 1 (Synchrotron SOLEIL). Diffraction was observed to a resolution of 2.7 Å (figure 2, Supplementary Information). Ten images were taken at room temperature, with 0.1s exposure each, before crystal deterioration. Those diffraction data allowed us to determine the space group of the crystal, $P2_12_12_1$, and the lattice parameters (a = 57.33 Å; b = 83.03 Å; c = 106.87 Å). When XRD is carried out under cryogenic conditions, the same space group is described for QR2 crystals, and the lattice parameters are a = 56.61 Å; b = 83.16 Å; c = 106.23 Å in accordance with the literature(Foster *et al.*, 1999). The strong X-ray damage to the crystal from these room-temperature measurements most likely explains why a complete data set was not obtained from one single crystal.

Microfluidics, however, can produce hundreds to thousands of droplets with identical composition. Thus, serial-crystallography at room temperature would yield a complete set of data for structural resolution with limited noticeable effects from radiation damage. This approach was used recently by Heymann(Heymann *et al.*, 2015) with a chip made of PDMS and COC (cyclic olefin polymer) or Kapton.

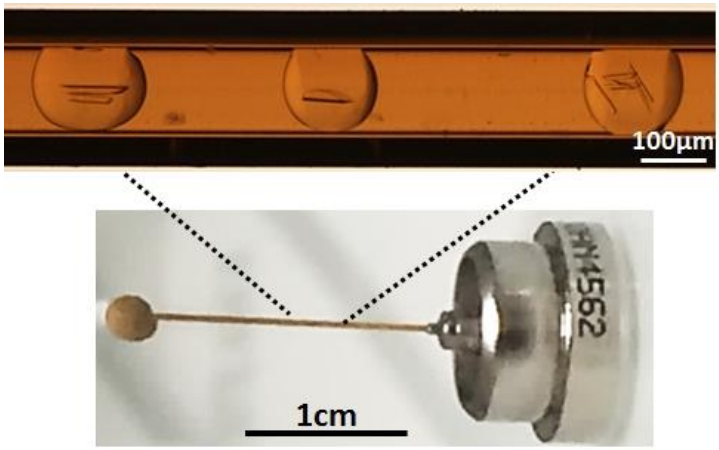

Figure 3. Photos of the silica tubing mounted on a magnetic base.

3.2. Ex situ XRD. Here, crystals were harvested from the Teflon tubing containing droplets. A droplet was deposited on a Micromesh™ (MiTeGen) using a high-precision micro-injector for flow control (Elveflow). The micro-injector and the MicroMesh™ are fixed to home-made micromanipulators for precise displacement in X, Y and Z (Grossier R. *et al.*, 2011) (figure 3, Supplementary Information). Crystals were placed singly on the MicroMesh™ (figure 4 and Supplementary Information: figure 4 and video 1) which was immediately extracted from the oil bath (FC70) and immersed in liquid nitrogen to cryogenize the crystals. Here, FC70 oil acted as a cryoprotectant, but crystals can be immersed in a drop of glycerol for cryoprotection. Then, XRD was carried out (table 1). By extracting the crystals without direct handling or mechanical stress and preparing the sample for diffraction studies under cryogenic conditions, we were able to collect a full data set at a resolution of 2.3Å (with or without glycerol). By determining structure from one single crystal, we identified electron density for the Flavin Adenine Dinucleotide (FAD) cofactor in the active site of QR2 (figure 5). Further studies should explore screening of QR2 co-crystallization with ligands for structure-based drug design. These first results confirm that the microfluidic approach yields crystallographic data of sufficient quality to allow us to judge whether or not the ligands bind to the active site.

Table 1

Data-collection statistics

Values in parentheses are for the highest resolution shell.

Diffraction Source	Proxima-I, SOLEIL
Wavelenght (Å)	0.97857
Temperature (K)	100
Detector	Dectris Pilatus 6M
Crystal-to-detector distance (mm)	440.50
Rotation range per image (°)	0.1
Total rotation range (°)	180
Exposure time per image (s)	0.1
Space group	$P2_12_12_1$
Unit-cell Parameters (Å, °)	a = 53.15, b = 81.62, c = 106.03 $\alpha = \beta = \gamma = 90$
Resolution (Å)	47.52-2.31 (2.37-2.31)
R_{merge} (%)	10.5 (68.7)
Completeness (%)	99.4 (93.8)
Total No. of reflections	87394
No. of unique reflections	20712 (1399)
Multiplicity	4.2 (3.9)
$\langle I/\sigma(I) \rangle$	8.0 (1.7)
Overall *B* factor from Wilson plot (Å^2)	26.99
$CC_{1/2}$	0.996 (0.687)

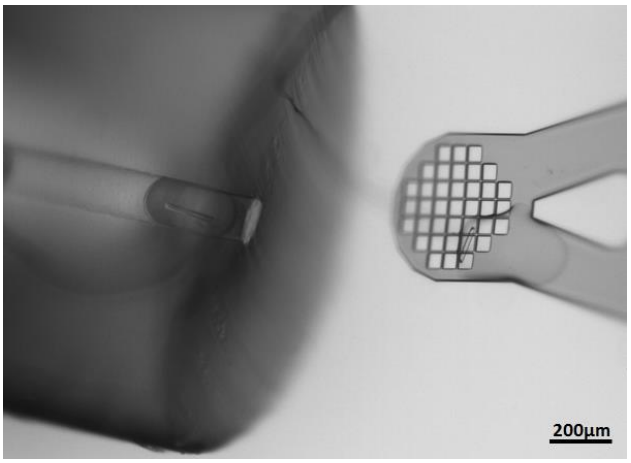

Figure 4. Photo of a crystal in a droplet deposited on the Micromesh^{TM}.

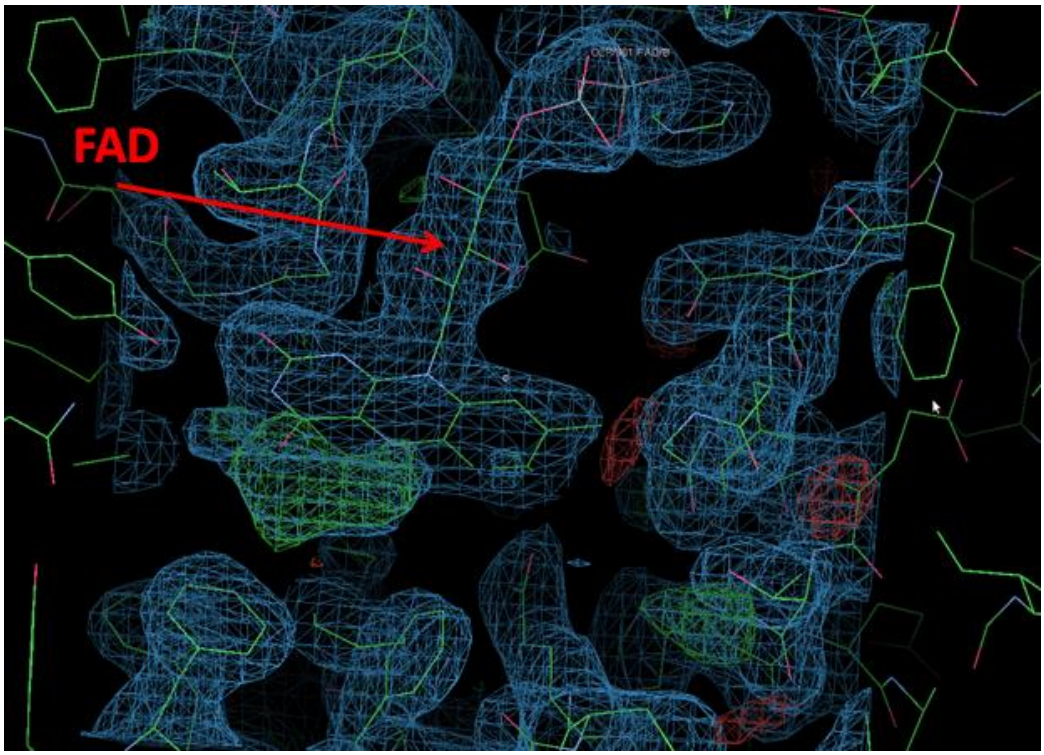

Figure 5. Electronic density map of the active site of QR2, with the FAD cofactor.

4. Conclusions

We present an application of a microfluidic platform developed in our group to the optimization of crystallization conditions of the pharmaceutical protein QR2. The resulting crystals were characterized by both in situ and ex situ X-ray diffraction.

Acknowledgments

We thank the Institut de Recherche Servier for financial support. We thank T. Bactivelane (CINaM), M. Lagaize (CINaM) and M. Audiffren (ANACRISMAT) for technical assistance. We thank G. Sulzenbacher, S. Spinelli and P. Cantau (AFMB) for the transport of the crystals and their support about crystallography. Experiments at Synchrotron SOLEIL were performed

under the *in house* proposal number 99150097. Results incorporated in this note received funding from the European Union's Horizon 2020 research and innovation programme under grant agreement No 708130.

References

Candoni N., Grossier R., Hammadi Z., Morin R. & Veesler S. (2012). *Protein & Peptide Letters* **19**, 714-724.

Dhouib, K., Khan Malek, C., Pfleging, W., Gauthier-Manuel, B., Duffait, R., Thuillier, G., Ferrigno, R., Jacquamet, L., Ohana, J., Ferrer, J.-L., Theobald-Dietrich, A., Giege, R., Lorber, B. & Sauter, C. (2009). *Lab on a Chip* **9**, 1412-1421.

Foster, C. E., Bianchet, M. A., Talalay, P., Zhao, Q. & Amzel, L. M. (1999). *Biochemistry* **38**, 9881-9886.

Fu, Y., Buryanovskyy, L. & Zhang, Z. (2008). *J Biol Chem* **283**, 23829-23835.

Gasteiger, E., Gattiker, A., Hoogland, C., Ivanyi, I., Appel, R. D. & Bairoch, A. (2003). *Nucleic Acids Research* **31**, 3784-3788.

Gerdts, C. J., Stahl, G. L., Napuli, A., Staker, B., Abendroth, J., Edwards, T. E., Myler, P., Van Voorhis, W., Nollert, P. & Stewart, L. J. (2010). *Journal of Applied Crystallography* **43**, 1078-1083.

Grossier R., Hammadi Z., Morin R., Magnaldo A. & veesler S (2011). *Applied Physics Letters* **98**, 091916-091913.

Guha, S., Perry, S. L., Pawate, A. S. & Kenis, P. J. A. (2012). *Sensors and Actuators B: Chemical* **174**, 1-9.

Hammadi, Z., Grossier, R., Zhang, S., Ikni, A., Candoni, N., Morin, R. & Veesler, S. (2015). *Faraday Discussions* **179**, 489-501.

Hansen, C. L., Classen, S., Berger, J. M. & Quake, S. R. (2006). *Journal of the American Chemical Society* **128**, 3142-3143.

Hashimoto, T. & Nakai, M. (2011). *Neurosci Lett* **502**, 10-12.

Heymann, M., Opathalage, A., Wierman, J. L., Akella, S., Szebenyi, D. M. E., Gruner, S. M. & Fraden, S. (2015). *IUCrJ* **2**, 601.

Horstman, E. M., Goyal, S., Pawate, A., Lee, G., Zhang, G. G. Z., Gong, Y. & Kenis, P. J. A. (2015). *Crystal Growth & Design*.

Khvostichenko, D. S., Schieferstein, J. M., Pawate, A. S., Laible, P. D. & Kenis, P. J. A. (2014). *Crystal Growth & Design*.

Leng J. & Salmon J.B. (2009). *Lab on a Chip* **9**, 24-34.

Li, L., Mustafi, D., Fu, Q., Tereshko, V., Chen, D. L., Tice, J. D. & Ismagilov, R. F. (2006). *Proceedings of the National Academy of Sciences* **103**, 19243-19248.

Maeki, M., Pawate, A. S., Yamashita, K., Kawamoto, M., Tokeshi, M., Kenis, P. J. A. & Miyazaki, M. (2015). *Analytical Chemistry* **87**, 4194-4200.

Maeki, M., Yoshizuka, S., Yamaguchi, H., Kawamoto, M., Yamashita, K., Nakamura, H., Miyazaki, M. & Maeda, H. (2012). *Analytical Sciences* **28**, 65-65.

Mazutis, L., Araghi, A. F., Miller, O. J., Baret, J.-C., Frenz, L., Janoshazi, A., Taly, V., Miller, B. J., Hutchison, J. B., Link, D., Griffiths, A. D. & Ryckelynck, M. (2009). *Analytical Chemistry* **81**, 4813-4821.

Nosjean, O., Ferro, M., Cogé, F., Beauverger, P., Henlin, J.-M., Lefoulon, F., Fauchère, J.-L., Delagrange, P., Canet, E. & Boutin, J. A. (2000). *Journal of Biological Chemistry* **275**, 31311-31317.

Pinker, F., Brun, M., Morin, P., Deman, A.-L., Chateaux, J.-F., Oliéric, V., Stirnimann, C., Lorber, B., Terrier, N., Ferrigno, R. & Sauter, C. (2013). *Crystal Growth & Design* **13**, 3333-3340.

Stojanoff, V., Jakoncic, J., Oren, D. A., Nagarajan, V., Navarro Poulsen, J.-C., Adams-Cioaba, M. A., Bergfors, T. & Sommer, M. O. A. (2011). *Acta Crystallographica Section F* **67**, 971-975.

van der Woerd, M., Ferree, D. & Pusey, M. (2003). *Journal of Structural Biology* **142**, 180-187.

Veesler, S., Ferté, N., Costes, M. S., Czjzek, M. & Astier, J. P. (2004). *Crystal Growth & Design* **4**, 1137-1141.
Yadav, M. K., Gerdts, C. J., Sanishvili, R., Smith, W. W., Roach, L. S., Ismagilov, R. F., Kuhn, P. & Stevens, R. C. (2005). *Journal of Applied Crystallography* **38**, 900-905.
Zhang, S., Ferté, N., Candoni, N. & Veesler, S. (2015). *Organic Process Research & Development* **19**, 1837-1841.
Zhang, S., Gerard, C. J. J., Ikni, A., Ferry, G., Vuillard, L. M., Boutin, J. A., Ferte, N., Grossier, R., Candoni, N. & Veesler, S. (2017). *Journal of Crystal Growth* **472**.

Crystallization using tubing microfluidics permits both in situ and ex situ X-ray diffraction

Charline J.J. Gerard[1], Gilles Ferry[2], Laurent M. Vuillard[2], Jean A. Boutin[2], Leonard Chavas[3], Tiphaine Huet[3], Nathalie Ferte[1], Romain Grossier[1], Nadine Candoni[1], Stéphane Veesler*[1]

[1]CINaM - CNRS, Aix-Marseille Université, Campus de Luminy, Case 913, F-13288 Marseille Cedex 09 fax : +334 91418916, email : veesler@cinam.univ-mrs.fr

[2]Institut de Recherches SERVIER, 125, chemin de ronde, F-78290 Croissy-sur-Seine.

[3]Synchrotron SOLEIL Proxima-I, Gif-sur-Yvette, France

Solubilities at 20°C are measured by equilibrating crystal-solution suspensions (initial volume of 40µL) over time as described in (Veesler *et al.*, 2004).
QR2 solutions are buffered at pH=8 (20mM Tris-HCl and 150mM NaCl). QR2 concentrations were checked by optical density measurements (Biochrom, Libra S22) using an extinction coefficient of 1.74 $mL.mg^{-1}.cm^{-1}$ at 280 nm (Gasteiger *et al.*, 2003).

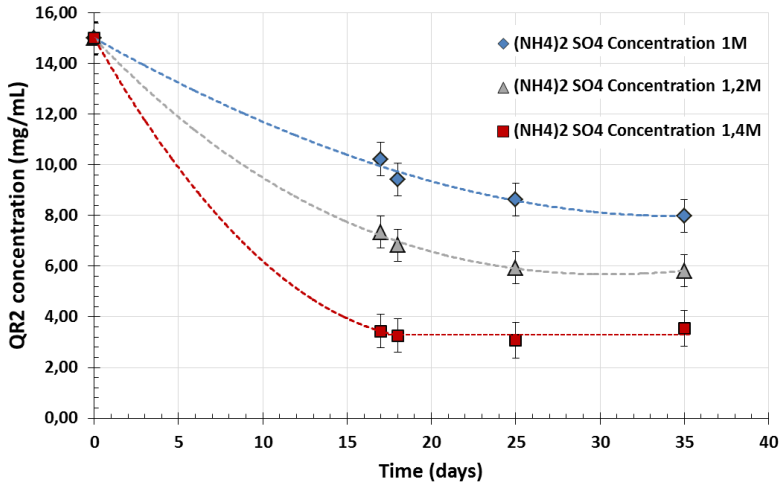

Figure 1. QR2 concentration vs time for 1, 1.2 and 1.4M $(NH_4)_2SO_4$ at 20°C. The plateaus after 20 days correspond to crystal-solution equilibrium, i.e. solubility. The solubility curve was plotted using a polynomial function of order 3.

Crystallography All diffraction data were recorded on a Pilatus-6M (Dectris®) detector at the beamline PROXIMA-1 from the Synchrotron SOLEIL (Paris, France), at the default energy of 12.67 keV, and sample-to-detector distance of 440.5 mm. For *in situ* measurements, the silica-tube containing the crystalline sample was adapted to a magnetic-base of the SPINE-geometry. Crystals were centred to the x-ray beam position using a 3-axis goniometer (SmarGon, SmarAct GmbH), either frozen under a cryo-jet set at 100K or kept at room temperature.

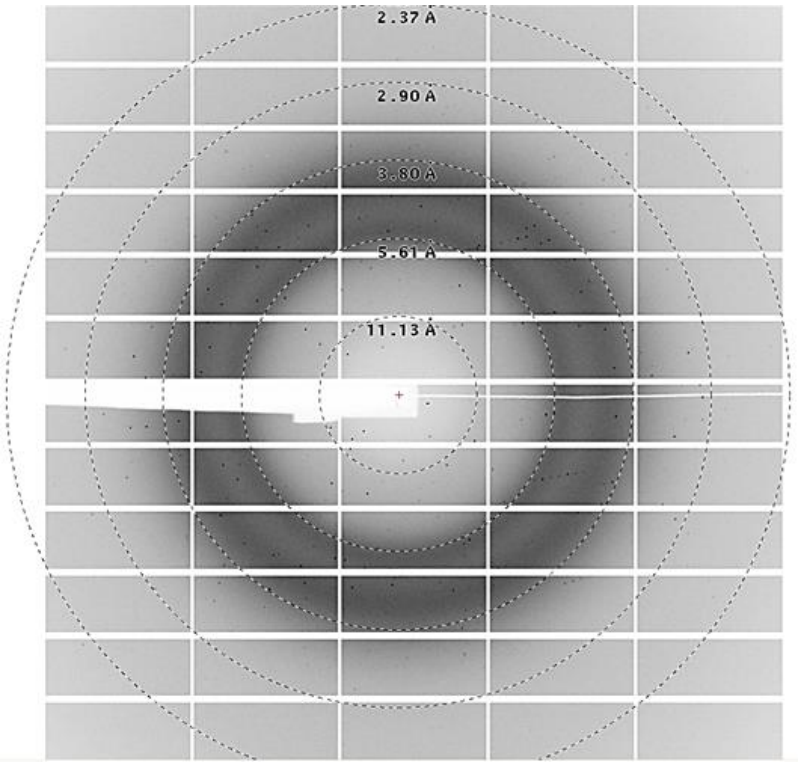

Figure 2. Diffraction pattern of QR2 taken at room temperature from the droplet inside the silica tube. The image illustrates the sum of ten wedged images collected each over an oscillation angle of 0.1º.

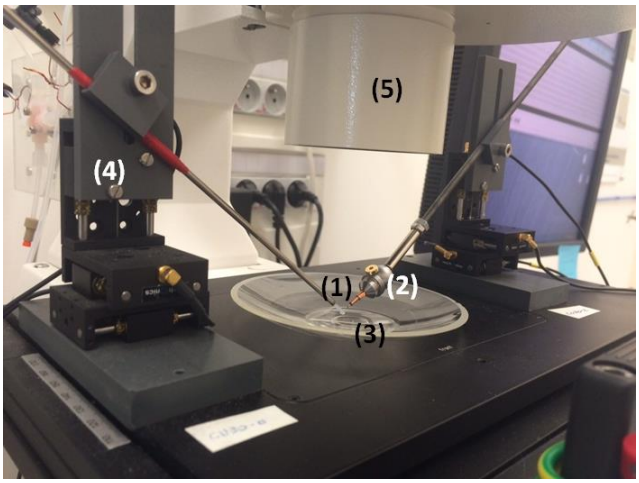

Figure 3. Photos of the micromanipulators (1): tube holder, (2): Micromesh™, (3): FC-70 oil, (4): XYZ miniature translation stage and (5): microscope.

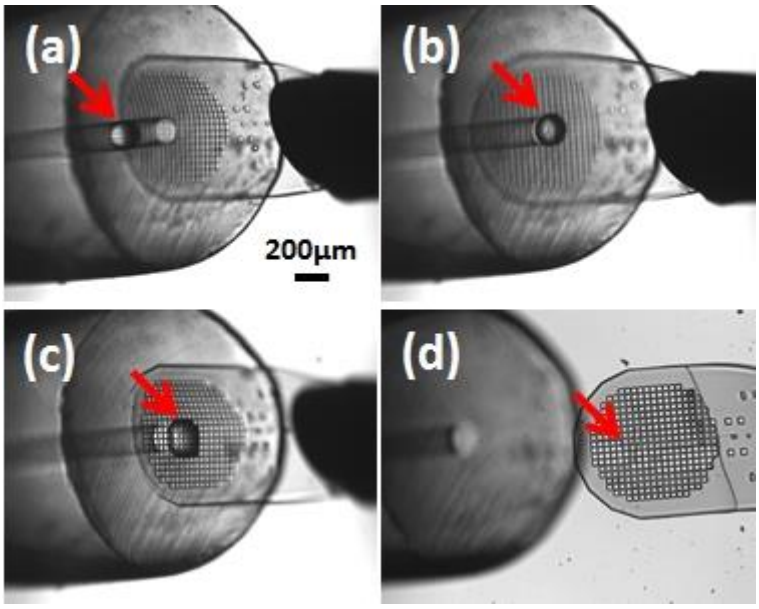

Figure 4. Time sequence of a droplet deposition on a Micromesh^{TM}.